FINITE ELEMENT RECONSTRUCTION OF DECOMPRESSIVE CRANIECTOMY

Máté Hazay[1], Annamária Varga[1], Eszter Nagy[1], Péter József Tóth[2], András Büki[2], Imre Bojtár[1]

[1] Faculty of Civil Engineering, Budapest University of Technology and Economics

[2] Department of Neurosurgery, University of Pécs

matehazay@hotmail.com

DOI: 10.17489/2018/2/08

Abstract

Traumatic brain injuries (TBIs) have a devastating global epidemiological importance since they contribute to the mortality and morbidity in the society with a considerably large extent. After TBI the injured brain tissue tends to swell leading to the increment of the intracranial pressure (ICP) which can cause serious neurological damage and death. Therefore, a main goal of the neurosurgical procedure is the reduction of ICP which is possible via decompressive craniectomy (DC). However, its optimal execution regarding the size and the location of the skull opening is controversial. In this paper the reconstruction of DC is performed by finite element (FE) simulations. The applied modelling strategy is presented and patient-specific FE models are constructed with different levels of anatomic details which can predict the post-operative response of the brain tissue for a given pre-operative state. These models are validated by reconstructing real life DC case, where the predicted displacements and ICP are compared to their observed value measured by neurosurgeons. Results confirm the applicability of the above described modelling procedure, implying that such models can be used to optimize DC in the future based on the biomechanical response of the highly deformable brain tissue.

Keywords: traumatic brain injuries, decompressive craniectomy, finite element simulations, intracranial pressure, Computer-Assisted Neurosurgery

Introduction

Traumatic brain injuries (TBIs) have a devastating global epidemiological importance since they contribute to the mortality and morbidity in the society with a considerably large extent.[1] One of the most important complications of TBIs is brain edema consisting of an abnormal fluid accumulation within the injured parenchyma and swelling of the brain. Brain swelling can lead to secondary injury by uncontrolled increment of intracranial pressure (ICP) which can cause serious neurological damage and death.[2-5] Accordingly, edema and its complications account for approximately 50% of death in patients with TBI,[6] therefore an important goal of the treatment is the reduction of ICP. Reduction of ICP can be achieved by decompressive craniectomy (DC) which can be used sometimes as a last-tier (i.e. an ultimate life-saving) surgical procedure.[7-10] In this operation a piece of skull is removed and the underlying dura mater is opened (Figure 1) in order to allow the brain to expand outside the skull bone resulting in a bulging deformation and the mitigation of ICP.[11,12]

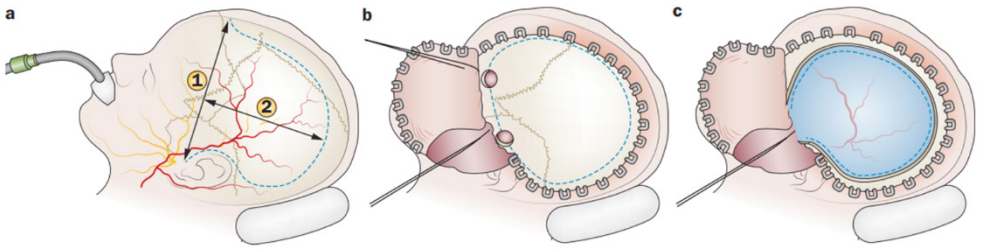

Figure 1. Main steps of decompressive craniectomy.
a) skin; *b)* skull and *c)* dura incision indicated by the dotted lines[13]

Despite the ICP reduction, axonal fibres are subjected to extreme stretching which is thought to contribute to an unfavourable neurological outcome for patients treated with DC.[14,15] Effective treatment of brain edema is challenging since the optimal execution of DC regarding the size and the location of skull opening is controversial[13] and the recommended treatment is based on clinical practice and personal experience.[16,17] Therefore, there is a need for developing new methods which can predict the biomechanical response of the swollen brain tissue. Accordingly, a long-term research goal can be formulated as performing a comprehensive optimization of DC based on the biomechanical response of the highly deformable brain tissue.[18]

Despite the enormous complexity of the brain, many aspects of its response can be described in purely mechanical terms, such as displacements, strains and stresses.[19] The latest trend in biomechanical research of brain injuries is performing finite element (FE) simulations[20-22] in order to determine the mechanical response of the human brain. There are several applications of biomechanical models in Computer-Assisted Neurosurgery[19] related to hydrocephalus[23-25] and image-guided surgery in case of tumour resection,[26,27] however, there is a lack of biomechanical research dealing with DC[28] since only a relatively few studies have been performed by now. Gao and Ang[18] presented the first 3D head model which was used to simulate ICP distribution and tissue deformation following DC. A poroelastic material model was applied for the brain tissue whose parameters were taken based on previous research, however they did not provide experimental validation of their model. Nevertheless, based on qualitative comparison of the calculated and observed brain deformations, it was concluded that FE models can be able to simulate DC. Furthermore, it was observed that the size of the craniectomy influences the reduction of ICP and the deformations of the tissue, thus it was hypothesized that an optimum should exist regarding the size of the skull opening. Moreover, the maximum stress regions were found near the craniectomy, which was confirmed by Holst et. al[29] via determining strains and water content in brain tissue by nonlinear medical image registration (MIR).

Later,[30] finite element models were developed with poroelastic tissue behaviour to reconstruct DC cases, and model validation was performed based on observed deformations of the brain tissue. Fletcher et. al[31] developed a simplistic FE model in order to reconstruct physical experiments performed on a surrogate model. Several material models were investigated for modelling the mechanical response of the brain tissue and it was found that the time-dependent material behaviour of the brain was not critical to the conditions at the early stages of loading when the peak strain occurred. Experiments[32] have shown that the mechani-

cal behaviour of the brain tissue is similar to the behaviour of filled elastomers, thus later finite element head model was developed[33] using Ogden's second order isotropic hyperelastic material model[34-36] for modelling the behaviour of the parenchyma. This model was not a patient-specific model since its geometric features were taken from the Collins Brain Atlas.[37] It was applied to determine maximum bulge displacement and volume exceeding a critical shear strain for different craniectomy types (unilateral, bilateral, bifrontal, etc).

As a summary of literature review, it is mentioned that during the optimization of DC the ICP and the strain of the parenchyma can be considered as objective functions which should be minimized. Previously mentioned models[18,30,33] were able to predict the deformations of the brain tissue, however ICP was not validated and in certain cases its value corresponding to the pre-operative (pre-op) state was used as natural boundary conditions at the boundaries of the parenchyma.[18] According to previous efforts,[18,33] the optimization of DC would include several simulations of DC which start from a given pre-op state and their execution is performed with different craniectomy sizes and locations, while resulting ICP and strains are monitored. This procedure would require the development of FE models which reliably predict not just strains but ICP of the parenchyma as well.

This paper presents a modelling strategy which can be used as a tool for the optimization of DC in the future. The development of 3D patient-specific head models are discussed in detail. By following these steps, two FE models are developed with different levels of anatomic details. These models are validated by reconstructing a real-life DC case where the predicted and observed ICP and deformations are compared.

Methods

According to previous research,[29] our modelling procedure starts from an initial reference state, where the geometry represents an approximated patient-specific healthy state. Since medical images of patients in the healthy state are not available in general, the healthy intracranial state is approximated by nonlinear MIR[29] using Computer Tomography (CT) images of healthy volunteers. However, it should be taken into account that the relative volume of ventricles (RVV) (i.e. the volume of lateral ventricles divided by the intracranial volume) has a relatively large variability among humans and ventricle volumes are age-dependent.[38] Therefore, in order to obtain an approximated average healthy state, three groups of volunteers were identified age-dependently (Group I for volunteers aged between 18-39 years, Group II for volunteers between 40-69 and Group III for volunteers elder than 70 years), and CT scans of 15 volunteers were used for each group respectively. The RVV was calculated for each volunteer by segmentation of CT images performed in 3D Slicer environment.[39] Afterwards, the obtained RVVs were considered as a statistical sample for each group, and one volunteer having the median RVV was chosen for each group respectively. With the application of this statistical procedure, working with a healthy volunteer having extremely small or extremely large ventricles was avoided.

The patient-specific healthy state is approximated by nonlinear MIR using B-splines[40] performed in 3D Slicer, where CT images of the chosen healthy volunteer *(Figure 2.a)* are morphed to the patient's CT images at the pre-op (i.e. injured) state *(Figure 2.b)* based on the patient's cranial shape.[29] The result of this transformation is a sequence of CT images where the cranial shape approximately agrees with the patient's cranial shape, but the shape of the intracranial anatomic parts represent an average healthy condition *(Figure 2.c)*.

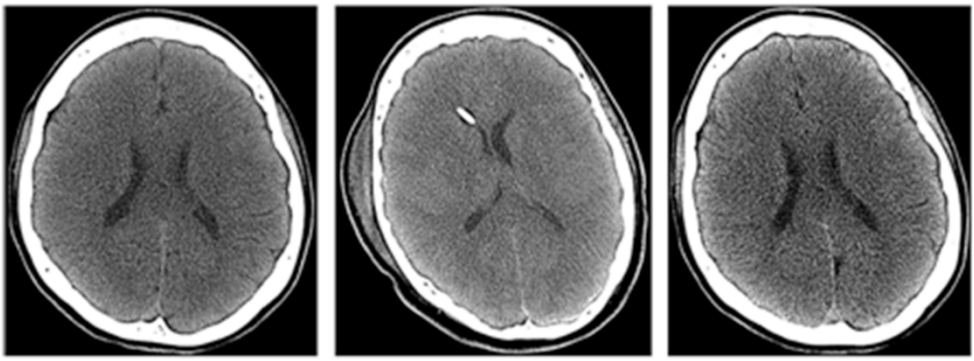

a) *b)* *c)*

Figure 2. Estimation of patient-specific healthy state by nonlinear medical image registration.
a) CT scan of a healthy volunteer; *b)* CT scan of the patient at the pre-op state;
c) CT scan of the approximated healthy condition

Segmentation of different parts of the human head can be performed on these CT images in 3D Slicer environment. In order to investigate the sensitivity of results due to the applied modelling level, two different models are created which represent different anatomic details.

The simplistic model (Model A) includes the parenchyma, the outer cerebrospinal fluid (CSF) space, the skull bone and dura mater (considered as one merged volume having a several magnitudes larger stiffness than the parenchyma), while the more complex model (Model B) contains the lateral ventricles and the falx cerebri as well. Due to convergence issues which were a barrier of previous research,[33] ventricles and the outer CSF space is not modelled by solid parts, but these are represented by cavities in the geometry. The supporting effect of CSF on the surface of the parenchyma is taken into account by a pressure load with 5 Hgmm intensity (approximating an initial healthy state) and an elastic spring support in order to model the increased ICP at the boundaries due to swelling. After the segmentation, surface models are obtained for each anatomic part which contain sharp edges and gaps, therefore their smoothing and correction are performed in Meshlab[41] by VCG reconstruction.[42] Afterwards, the smoothed surface models can be converted to 3D CAD geometry *(Figure 3.a-b)* which is performed in Ansys

a) *b)* *c)*

Figure 3. Geometry and mesh of the patient-specific FE model.
a) Geometry of the brain and the opened skull; *b)* Geometry of lateral ventricles;
c) FE mesh of the brain tissue and the falx cerebri

SpaceClaim[43] environment. The obtained geometry can be imported to Ansys Workbench[44] environment where the finite element model is developed *(Figure 3.c)*.

In order to separate FE mesh generation from the unimportant geometric features, a virtual topology[44] is constructed by generating virtual cells. Afterwards, a patch independent finite element mesh[44] is constructed consisting of tetrahedral finite elements for solid volumes and shell elements for the falx *(Figure 3.c)*. In accordance with previous research,[33] parenchyma is considered as an isotropic, hyperelastic material modelled by a second-order Ogden material model[34-36] whose strain energy function U is shown in Equation 1:

$$U = \sum_{i=1}^{2} \frac{2\mu_i}{\alpha_i^2}\left(\lambda_1^{\alpha_i} + \lambda_2^{\alpha_i} + \lambda_3^{\alpha_i} - 3\right), \qquad (1)$$

where parameters and describe the shear modulus, parameters and characterize the strain hardening effect *(Table 1)* and are the deviatoric principal stretches. The mechanical behaviour of the skull and the falx is simulated by a linear elastic material model used in previous model[45] whose Young's modulus and Poisson's ratio are listed in *Table 1.*

According to previous research,[29] modelling of DC consists of two stages. In the first stage the brain swelling is modelled, i.e. an injured pre-op state is obtained from the initial healthy state. Brain swelling is obtained by artificial thermal expansion[33] of the parenchyma leading to the increased ICP in the pre-op state. The distribution of the thermal loading depends on the actual injury type and can be estimated by the Hounsfield-unit[46-48] obtained from CT images.

In the current case, edema was modelled by a uniformly distributed thermal loading of the parenchyma supplemented by an additional local thermal expansion which causes an increased ICP near the focal contusion of the tissue. The magnitude of the thermal loading is determined by a calibration procedure, where the applied temperature is calculated by the false position method[49] based on the equality of the observed and predicted ICP of the parenchyma at the pre-op state near the lateral ventricles. Finite element nodes of the skull and the outer edges of the falx are rigidly supported against translational displacements, while the surface of the parenchyma is elastically supported by spring elements representing the supporting effect of CSF. Furthermore, a frictionless contact is established between the skull and the parenchyma, and the brain and the falx.

In the second stage DC is performed, thus the post-op state is obtained from the pre-op state by removing a portion of the skull and dura via prescribed displacements. In this step the supporting effect of CSF near the skull opening is neglected and the bulging deformation of parenchyma is obtained.

Anatomic part	Material model	Material parameters	
Skull	Linear elastic	E = 15000 MPa	ν = 0,22
Dura mater and falx cerebri	Linear elastic	E = 31,5 MPa	ν = 0,45
Brain tissue	Hyperelastic	μ_1 = 1,044 kPa	α_1 = 4,309
		μ_2 = 1,183 kPa	α_2 = 7,736

Table 1. Applied material models and parameters

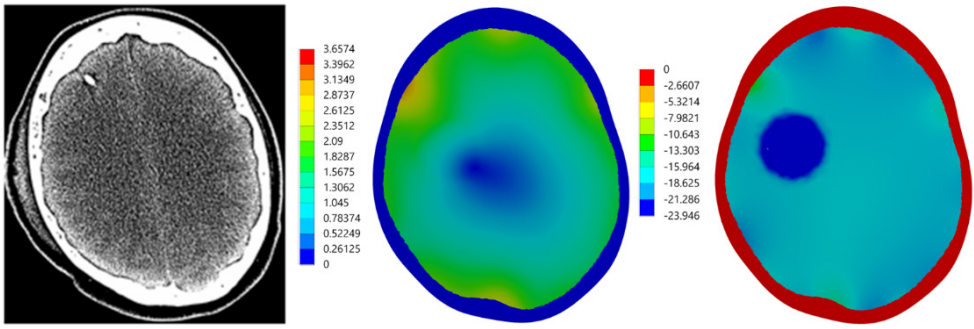

a) *b)* *c)*

Figure 4. Observed and simulated results (obtained by Model A) at the pre-op state.
a) CT scan; *b)* simulated displacements; *c)* simulated ICP

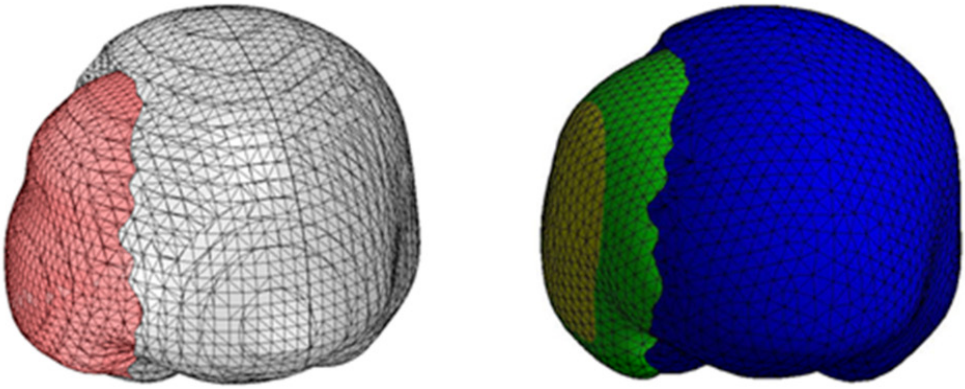

a) *b)*

Figure 5. Observed *(a)* and simulated *(b)* bulging deformation of the brain tissue

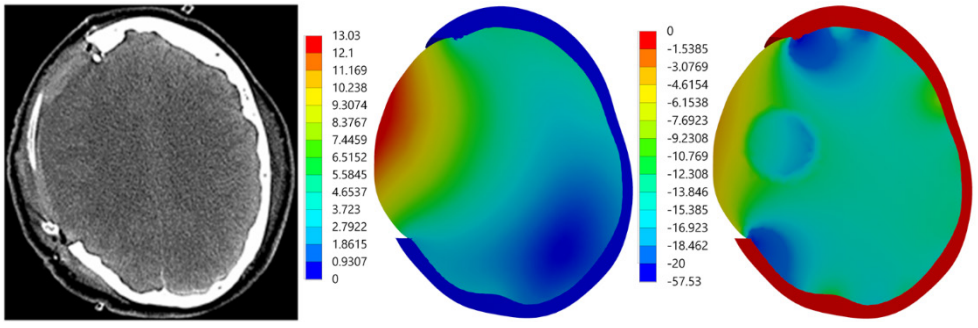

a) *b)* *c)*

Figure 6. Observed and simulated results (obtained by Model A) at the post-op state.
a) CT scan; *b)* simulated displacements; *c)* simulated ICP

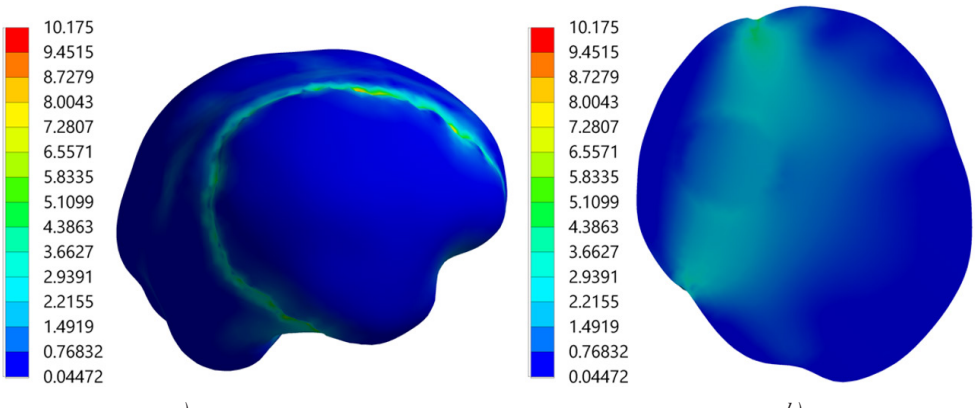

Figure 7. Von Mises stresses of the parenchyma [kPa].
a) stress peaks near the perimeter of craniectomy; *b)* stresses in an axial section

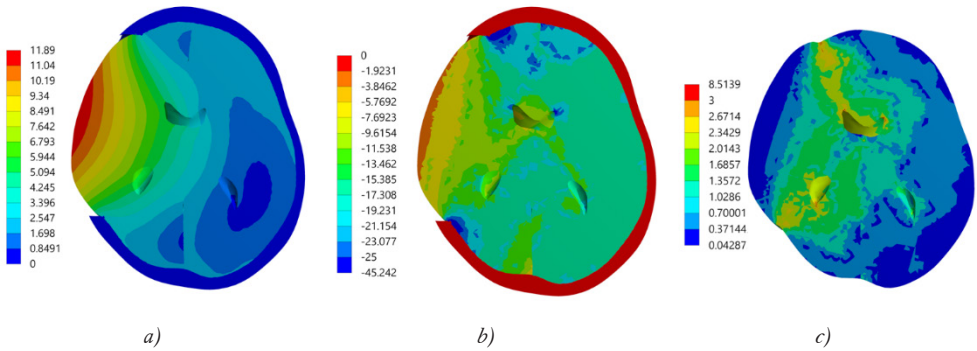

Figure 8. Predicted results at the post-op state obtained by Model B.
a) displacements; *b)* ICP; *c)* von Mises stresses

Results

In this section, results of the model validation are shown corresponding to the reconstruction of a real-life DC case. Simulated deformations and ICP of the parenchyma obtained by Model A at the pre-op state is shown in *Figure 4.b-c.*

Afterwards, the simulation of skull removal was performed and a bulging deformation was obtained *(Figure 5.b)* which is similar to the observed deformations (which was obtained by the segmentation) of the brain tissue *(Figure 5.a)*. Results at the post-op state in terms of displacements and ICP (obtained by Model A) are shown in *Figure 6.b-c.*

Von Mises stresses of the parenchyma at the post-op state obtained by Model A is shown in *Figure 7.*

Results obtained by Model B corresponding to the post-op state are shown in *Figure 8.*

Beside the qualitative comparison, a quantitative analysis was also performed of the predicted and observed results (Table 2). The simulated ICP values show the average ICP obtained in finite elements which belong to a sphere with 5 cm diameter around the ventricles.

	Measured	Predicted by Model A	Predicted by Model B
Max. displacement [mm]	≈17	13,03	11,89
Pre-op ICP [Hgmm]	18	18,10	18,07
Post-op ICP [Hgmm]	12	12,19	14,52

Table 2. Quantitative comparison of observed and predicted results

Discussion

In this paper a finite element modelling strategy of decompressive craniectomy has been detailed and corresponding patient-specific models were constructed with different anatomic details. Model validation has been performed by reconstructing a real-life case where qualitative and quantitative comparison of simulated and observed displacements and ICP were made. Resulting from the calibration procedure, ICP near the lateral ventricles at the pre-op state *(Figure 4.c)* fits well to its measured value *(Table 2)*. A qualitative analysis of bulging displacements based on results of FE simulations *(Figure 5, Figure 6.a-b, Figure 8.a)* showed that the predicted displacements of the parenchyma approximates well the observed deformations in case of both models.

The quantitative comparison showed that the difference in terms of maximal displacements between predicted and observed results is about 4-6 mm *(Table 2)*, which is considered here as an acceptable agreement. According to our results corresponding to the post-op state *(Figure 6.c; Figure 8.b, Table 2)* the simulated ICP values obtained by both models fit relatively well to the measurements performed at the clinic. Results of the von Mises stresses obtained by Model A *(Figure 7.a)* confirm that large stresses and strains occur near the perimeter of the craniectomy which could be responsible of poor neurological outcome. However, stress and strain peaks near the lateral ventricles whose existence was observed in previous study[29] could only be predicted by Model B *(Figure 7.b, Figure 8.c)*, therefore it is concluded that the optimization in the future must be performed on models where lateral ventricles are included. Based on results obtained by Model B *(Figure 8, Table 2)*, the currently applied modelling strategy can be an adequate tool for modelling DC. Following this modelling procedure, validated patient-specific FE models can be applied to optimize decompressive craniectomy in the future, by performing virtual experiments with different craniectomy size and locations while ICP and strains or stresses of the parenchyma are monitored.

REFERENCES

1. *Frieden TR, Houry D, Baldwin G.* Report to Congress on Traumatic Brain Injury in the United States: Epidemiology and Rehabilitations. CDC Report, 2010. Available from: https://www.cdc.gov/traumaticbraininjury/pdf/tbi_report_to_congress_epi_and_rehab-a.pdf.
2. *Chambers IR, Treadwell L, Mendelow AD.* Determination of threshold levels of cerebral perfusion pressure and intracranial pressure in severe head injury by using receiver-operating characteristic curves: an observational study in 291 patients. J Neurosurg 2001 Mar;94(3): 412-6.
3. *Balestreri M, Czosnyka M, Hutchinson PJ, Steiner LA, Hiler M, Smielewski P, Pickard JD.* Impact of intracranial pressure and cerebral perfusion pressure on severe disability and mortality after head injury. Neurocrit Care 2006;4(1): 8-13.
4. *Farahvar A, Gerber LM, Chiu Y-L, Härtl R, Froelich M, Carney N, Ghajar J.* Response to intracranial hypertension treatment as a predictor of death in patients with severe traumatic brain injury. J Neurosurg 2011 May;114(5): 1471-8.

5. *Badri S, Chen J, Barber J, Temkin NR, Dikmen SS, Chesnut RM, Deem S, Yanez ND, Treggiari MM.* Mortality and long-term functional outcome associated with intracranial pressure after traumatic brain injury. Intensive Care Med 2012 Nov;38(11): 1800-9.
6. *Marmarou A.* Pathophysiology of traumatic brain edema: current concepts. Acta Neurochir Suppl 2003;86: 7-10.
7. *Polin RS, Shaffrey, ME, Bogaev CA, Tisdale N, Germanson T, Bocchicchio B, Jane JA.* Decompressive bifrontal craniectomy in the treatment of severe refractory posttraumatic cerebral edema. Neurosurgery 1997 Jul;41(1): 84-94.
8. *Whitfield PC, Patel H, Hutchinson PJ, Czosnyka M, Parry D, Menon D, Pickard JD, Kirkpatrick PJ.* Bifrontal Decompressive Craniectomy in the Management of Posttraumatic Intracranial Hypertension. BR J Neurosurg 2001;15(6): 500-7.
9. *Aarabi B, Hesdorffer DC, Ahn ES, Aresco C, Scalea TM, Eisenberg HM.* Outcome following decompressive craniectomy for malignant swelling due to severe head injury. J Neurosurg 2006 Apr;104(4): 469-79.
10. *Honeybul S, Ho KM, Lind CR, Gillett GR.* Observed versus predicted outcome for decompressive craniectomy: a population-based study. J Neurotrauma 2010 Jul;27(7): 1225-32.
11. *Timofeev I, Czosnyka M, Nortje J, Smielewski P, Kirkpatrick P, Gupta A, Hutchinson PJ.* Effect of decompressive craniectomy on intracranial pressure and cerebrospinal compensation following traumatic brain injury. J Neurosurg 2008 Jan;108(1): 66-73.
12. *Bor-Seng-Shu E, Figueiredo EG, Amorim RL, Teixeira MJ, de Oliveira MM, Panerai RB.* Decompressive craniectomy: a meta-analysis of influences on intracranial pressure and cerebral perfusion pressure in the treatment of traumatic brain injury. J Neurosurg 2012 Sep;117(3): 589-96.
13. *Kolias AG, Kirkpatrick PJ, Hutchinson PJ.* Decompressive craniectomy: past, present and future. Nature Reviews Neurology 2013 Jul;9: 405-15.
14. *Cooper DJ, Rosenfeld JV, Murray L, Arabi YM, Davies AR, D'Urso P, Kossmann T, Ponsford J, Seppelt I, Reilly P, Wolfe R.* Decompressive craniectomy in diffuse traumatic brain injury. New England Journal of Medicine 2011 Apr;364(16): 1493-502.
15. *Stiver SI.* Complications of decompressive craniectomy for traumatic brain injury. Neurosurg Focus 2009 Jun;26(6): E7.
16. *von Holst H. Traumatic brain injury. In: Feigin VL, Bennett DA, editors.* Handbook of Clinical Neuroepidemiology. New York: Nova Science Publishers 2007: 197-232.
17. *Rabinstein AA.* Treatment of Cerebral Edema. Neurologist 2006 Mar;12(2): 59-73.
18. *Gao CP, Ang BT.* Biomechanical modelling of decompressive craniectomy in traumatic brain injury. In: Steiger HJ, editor. Acta Neurochirurgica Supplements. Vienna: Springer. Acta Neurochirurgica Supplementum 2008;102: 279-82.
19. *Miller K, Wittek A, Joldes G.* Biomechanical Modeling of the Brain for Computer-Assisted Neurosurgery. In: Miller K, editor. Biomechanics of the Brain. New York: Springer,2011: 111-136.
20. *Takhounts EG, Eppinger RH, Campbell JQ, Tannous RE, Power ED, Shook LS.* On the development of the SIMon Finite Element Head Model. 47th Stapp Car Crash Journal 2003 Oct;47: 107-133.
21. *Kleiven S.* Predictors for traumatic brain injuries evaluated through accident reconstruction. Stapp Car Crash Journal 2007 Oct;51: 81-114.
22. *Post A, Kendall M, Koncan D, Cournoyer J, Hoshizaki TB, Gilchrist MD, Brien S, Cusimano MD, Marshall S.* Characterization of Persistent Concussive Syndrome Unsing Injury Reconstruction and Finite Element Modelling. J Mech Behav Biomed Mater 2014 Aug;41: 325-35.
23. *Cheng S.* The role of brain tissue mechanical properties and cerebrospinal fluid flow in the biomechanics of the normal and hydrocephalic brain. PhD Thesis, Graduate School of Biomedical Engineering, University of New South Wales 2006.
24. *Miller K, Taylor Z.* Reassessment of brain elasticity for analysis of biomechanisms of hydrocephalus. J Biomech 2004 Aug;37(8): 1263–9.
25. *Kim H, Jeong EJ, Park DH, Czosnyka Z, Yoon BC, Kim K, Czosnyka M, Kim DJ.* Finite element analysis of periventricular lucency in hydrocephalus: extravasation or transependymal CSF absorption? J Neurosurg 2016 Feb;124(2): 334-41.
26. *Joldes G, Wittek A, Couton M, Warfield S, Miller K.* Real-time prediction of brain shift using nonlinear finite element algorithms. In: Proceedings of the International Conference on Medical Image Computing and Computer-Assisted Intervention, 2009 Sep 20-24, London, United Kingdom 2009: 300–7.
27. *Wittek A, Hawkins T, Miller K.* On the unimportance of constitutive models in computing brain deformation for image-guided surgery. Biomech. Model. Biomech Model Mechanobiol 2009 Feb;8(1): 77–84.
28. *Goriely A, Geers GDM, Holzapfel GA, Jayamohan J, Jérusalem A, Sivaloganathan S, Squier W, van Dommelen JA, Waters S, Kuhl E.* Mechanics of the brain: perspectives, challenges and opportunities. Biomech Model Mechanobiol 2015 Oct;14(5): 931–65.
29. *von Holst H, Li X, Kleiven S.* Increased strain levels and water content in brain tissue after decompressive craniotomy. Acta Neurochir 2012 Sep;154(9): 1583-93.

30. *Li X, von Holst H.* Finite Element Modeling of Decompressive Craniectomy (DC) and its Clinical Validation. Advances in Biomedical Science and Engineering 2015 Mar;2(1): 1-9.

31. *Fletcher TL, Kolias AG, Hutchinson PJA, Sutcliffe MPF.* Development of a Finite Element Model of Decompressive Craniectomy. PLoS ONE 2014 Jul;9(7): e102131.

32. *Franceschini G, Bigoni D, Regitnig P, Holzapfel GA.* Brain tissue deforms similarly to filled elastomers and follows consolidation theory. Journal of the Mechanics and Physics of Solids 2006 Dec;54(12): 2592-620.

33. *Fletcher TL, Wirthl B, Kolias AG, Adams H, Hutchinson PJA, Sutcliffe MPF.* Modelling of Brain Deformation After Decompressive Craniectomy. Annals of Biomedical Engineering 2016 Dec;44(12): 3495-509.

34. *Ogden RW.* Large deformation isotropic elasticity - on the correlation of theory and experiment for incompressible rubberlike solids. Proceedings of the Royal Society of London. Series A, Mathematical and Physical Sciences 1972 Feb;326(1567): 565-84.

35. *Ogden RW.* Recent Advances in the Phenomenological Theory of Rubber Elasticity. Rubber Chemistry and Technology, 1986 Jul;59(3): 361-83.

36. *Ogden RW, Roxburgh DG.* A pseudo-elastic model for the Mullins effect in filled rubber. Proceedings of the Royal Society of London. Series A, Mathematical and Physical Sciences 1999 Aug; 455(1988): 2861-77.

37. *Collins DL, Zijdenbos AP, Kollokian V, Sled JG, Kabani NJ, Holmes CJ, Evans AC.* Design and construction of a realistic digital brain phantom. IEEE Trans Med Imaging 1998 Jun;17(3): 463-8.

38. *Kruggel F.* MRI-based volumetry of head compartments: normative values of healthy adults. Neuroimage 2006 Mar;30(1): 1-11.

39. *Pieper S, Halle M, Kikinis R. 3D Slicer.* Proceedings of the 2nd IEEE International Symposium on Biomedical Imaging: Nano to Macro, 2004 Apr 15-18, Arlington, VA, USA 2004 1: 632-5.

40. *Gu S, Meng X, Sciurba FC, Wang C, Kaminski N, Pu J.* Bidirectional Elastic Image Registration Using B-Spline Affine Transformation. Comput Med Imaging Graph 2014 Jun;38(4): 306-14.

41. *Cignoni P, Callieri M, Corsini M, Dellepiane M, Ganovelli F, Ranzuglia G.* MeshLab: an Open-Source Mesh Processing Tool. Proceedings of the 6th Eurographics Italian Chapter Conference, 2008 Jul 2-4, Salermo, Italy 2008: 129-36.

42. *Nabil M, Betró M, Metwally MN.* 3D reconstruction of ancient egyptian rock-cut tombs: the case of M.I.D.A.N.05. In the Proceedings of the XXIV International CIPA Symposium, 2013 Sep 2-6, Strasbourg, France 2013: 443-7.

43. ANSYS® Academic Research, Release 18.0, SpaceClaim User's Guide, ANSYS, Inc.

44. ANSYS® Academic Research, Release 18.0, ANSYS Workbench User's Guide, ANSYS, Inc.

45. *Horgan TJ, Gilchrist MD.* The creation of three-dimensional finite element models for simulating head impact biomechanics. IJCrash 2003 Jan;8(4): 353-66.

46. *Ito U, Reulen HJ, Tomita H, Ikeda J, Saito J, Maehara T.* Formation and propagation of brain oedema fluid around human brain metastases. A CT study. Acta Neurochir 1988 Mar;90(1-2): 35-41.

47. *Rieth KG, Fujiwara K, Di Chiro G, Klatzo I, Brooks RA, Johnston GS, O'Connor CM, Mitchell LG.* Serial measurements of CT attenuation and specific gravity in experimental cerebral edema. Radiology 1980 May;135(2): 343–8.

48. *Rózsa L, Grote EH, Egan P.* Traumatic brain swelling studied by computerized tomography and densitometry. Neurosurg Rev, 1989 Apr;12(2): 133–40.

49. *Press WH, Flannery BP, Teukolsky SA, Vetterling WT. Secant Method, False Position Method, and Ridders' Method. In: Numerical Recipes in FORTRAN: The Art of Scientific Computing, 2nd ed. Cambridge: Cambridge University Press 1992: 347-52.*

This research was supported by the ÚNKP-17-3-1 New Excellence Program and the BME-Biotechnology FIKP grant (BME FIKP-BIO) of the Ministry of Human Capacities.

Máté Hazay
Faculty of Civil Engineering , Budapest University of Technology and Economics
H-1111, Budapest, Műegyetem rkp. 3., T. bldg. III.,
Tel.: (+36) 30 634-4721